Polymer Journal (2018) 50:431–438
https://doi.org/10.1038/s41428-018-0029-7

ORIGINAL ARTICLE

The degree of crystallinity and segmental mobility in interpenetrating spherulites of poly(butylene succinate) and poly (ethylene oxide)

Takayuki Ikehara[1] · Toshiyuki Kataoka[1]

Received: 12 December 2017 / Revised: 17 January 2018 / Accepted: 18 January 2018 / Published online: 21 February 2018

Abstract

The influence of poly(butylene succinate) (PBS) crystals on the crystallinity of poly(ethylene oxide) (PEO) in PBS/PEO blends, which exhibit interpenetrating spherulites, was examined. The degree of crystallinity, ϕ, of each component was obtained by pulsed nuclear magnetic resonance (NMR). The value of ϕ of PBS exhibited a maximum that was larger than that of the homopolymer, whereas PEO exhibited a nearly constant ϕ throughout the composition. The dilution effect, order of crystallization, and change in the glass transition temperature upon blending were discussed as factors contributing to the ϕ. PEO exhibited an apparent secondary crystallization, where ϕ gradually increased and the mobility of the chain segments was suppressed. The secondary process of PBS, on the other hand, was nearly negligible.

Introduction

The miscible blends and block copolymers comprised of semicrystalline polymers often show the formation of interpenetrating spherulites (IPS), i.e., spherulitic growth of one component that continues to grow inside the spherulites of the other component [1–32]. The constituent with a lower melting point usually has a higher crystallinity and growth rate in the blends reported so far.

The formation process of IPS is classified into two types: the simultaneous and stepwise growth of spherulites. In the simultaneous growth process, both substances, which generally have a difference in the melting point, T_m, of approximately 30 K or less, simultaneously develop spherulites, and IPS are formed after the growth fronts of the different components contact each other [1–18]. In the stepwise process, which is generally observed when the T_m difference is approximately 50 K, the spherulites with a higher T_m grow first and fill the whole volume. Then, the spherulites of the other component nucleate and develop inside the existing spherulites [16–32].

When IPS are formed, the crystals of the penetrated spherulites may suppress the crystallization of the penetrating spherulites, which develop in restricted regions such as the interlamellar and interfibrillar regions [11, 22–24, 33]. Such suppression may result in a reduced degree of crystallinity, which is one of the most fundamental properties of semicrystalline polymers from scientific and engineering viewpoints. However, such effects have not been examined sufficiently thus far. The morphological formations and crystallization kinetics have mainly been investigated in the papers on IPS published so far.

The only work that has focused on the degree of crystallinity in IPS is, to the best of our knowledge, a paper on blends of poly(ethylene succinate) (PES) and poly(ethylene oxide) (PEO) using pulsed nuclear magnetic resonance (pulsed NMR) [34]. Nevertheless, the simultaneous crystallization of PES and PEO made the evaluation of the crystal content and the degree of crystallinity less precise. Moreover, the two types of PEO crystals in the simultaneous process, i.e., those that had grown inside and outside the PES spherulites, also made discussing the influences of the PES crystals difficult. Only the former type of PEO spherulites is influenced by the PES crystals. Furthermore, no discussion on the spin-spin relaxation time, T_2, or the mobility of the chain segments was presented.

✉ Takayuki Ikehara
ikehara@kanagawa-u.ac.jp

[1] Department of Material and Life Chemistry, Faculty of Engineering, Kanagawa University, 3-27-1, Rokkakubashi, Kanagawa-ku, Yokohama 221-8686, Japan

The difficulties described in the previous paragraph can be resolved by investigating IPS that exhibit stepwise spherulitic growth. The blends of poly(butylene succinate) (PBS) and PEO represent such a system, and PBS is the higher-T_m component [19–24]. All PEO spherulites grow inside the PBS spherulites under the influence of the PBS crystals, and the amount of the crystals of the two substances can be separately determined. PBS/PEO blends exhibit homogeneous melts above T_m. At elevated temperatures, the melts are reported to undergo phase separation [35]. The phase diagram has a lower critical solution temperature that is substantially higher than the T_m of PBS.

Pulsed NMR is an effective method to determine the absolute values of the degree of crystallinity based on the number of protons by analyzing the spin-spin relaxation [34, 36–42]. The degree of crystallinity can be obtained from the magnitude of the Gaussian or Weibull function with a T_2 on the order of 10^{-5} s. The crystallization process can also be analyzed if the crystallization rate is sufficiently slower than the acquisition rate of the data [34, 36, 37]. Slow processes such as secondary crystallization can also be analyzed by pulsed NMR, whereas the small heat flow of the secondary process makes an analysis by differential scanning calorimetry very difficult.

The aim of this paper is to discuss the degree of crystallinity in PBS/PEO blends, which exhibit stepwise spherulitic growth in the IPS formation process. The degree of crystallinity of each component in the blends is derived from the crystal content obtained by pulsed NMR. The mobility of the chain segments and the factors contributing to the degree of crystallinity of the constituents are discussed.

Experimental

PBS ($M_n = 43{,}000$, $M_w = 84{,}000$, $T_m^\circ = 120$ °C, $T_g = -32$ °C) and PEO ($M_n = 70{,}000$, $M_w = 404{,}000$, $T_m^\circ = 65$ °C, $T_g = -65$ °C) were purchased from Sigma-Aldrich Company. Weighed PBS and PEO were dissolved in chloroform. A solution of approximately 1 wt.% was then dried in a fume hood for 3 days and then under a vacuum at 35 °C for 3 days. The weight ratios of the blends were PBS/PEO = 2/8, 3/7, 4/6, and 5/5. Hereafter, the first and second digits indicate the contents of PBS and PEO, respectively, in the blends.

The pulsed NMR measurements were carried out with a JNM-25 MU (Jeol) as follows. The solid samples in NMR tubes with a diameter of 10 mm were first melted in a dry block bath at 120 °C before they were quickly transferred into the NMR probe, whose temperature was controlled at the crystallization temperature, T_c. The spin-spin relaxation signals of ^{1}H at a resonant frequency of 25 MHz were repeatedly collected using a solid echo pulse sequence [43]. Four decay signals were averaged for the noise reduction. The details of the pulsed NMR measurements can be found in other papers [34, 36, 37].

The spin-spin relaxation decay, I, of the blends was decomposed into Weibull and exponential functions after the onset of crystallization, as

$$I(t) = A_1 \exp\left[-\frac{1}{\mu}\left(\frac{t}{T_2^{(1)}}\right)^{\mu}\right] + A_2 \exp\left(-\frac{t}{T_2^{(2)}}\right) \quad (1)$$

where A_i and $T_2^{(i)}$ are the amplitude and spin-spin relaxation time of component i, respectively, t is the relaxation time, and μ is the parameter of the Weibull function. Components 1 and 2 were assigned to the immobile crystalline and mobile amorphous parts with T_2 values typically on the order of 10^{-5} s and 10^{-3}–10^{-4} s, respectively. The fractional amount of the crystals, f, based on the number of protons is defined by

$$f = A_1/(A_1 + A_2) \quad (2)$$

The crystallization process was also monitored using a polarized optical microscope (Olympus, BX51) equipped with a temperature controller (Linkam, 10002 and TMS-600) and a digital camera (Roper Scientific, CoolSNAP5.0). The blend samples, whose film thickness was approximately 10 μm, were placed between two optical glass plates. They were melted at 140 °C for approximately 3 min and then quenched to the desired T_c.

Results and discussion

The polarized optical micrographs of the crystallization process at 50 °C in a 3/7 blend are displayed in Fig. 1. The spherulites of PBS, which is the higher-T_m component, nucleated first and filled the whole sample, as shown in Fig. 1a. Then, PEO nucleated in the spherulites of PBS and grew with a spherulitic shape, as shown in Fig. 1b, c. The ranges of the T_c and the blend composition for the pulsed NMR measurements were determined by optical microscopy to ensure the crystallization rate was suitable for the pulsed NMR measurements.

Figure 2 shows an example of a normalized spin–spin relaxation function, I. The magnitude of the fast-decay component, which was fitted to the Weibull function, indicates the fraction of the crystals based on the number of protons.

The changes in f and T_2 for the crystalline component with a crystallization time, t, for the two homopolymers are indicated in Fig. 3, which was obtained by curve fitting the relaxation functions repeatedly acquired at different t. The increase in f represents the primary crystallization, namely,

Fig. 1 The polarized optical micrographs of the crystallization process in a PBS/PEO = 3/7 blend at 50 °C. **a** Completion of the growth of PBS spherulites, which filled the whole volume, and (**b**, **c**) nucleation and growth of a PEO spherulite inside the PBS spherulites. The pictures in (**b**) and (**c**) were taken 10 s and 31 s after (**a**), respectively

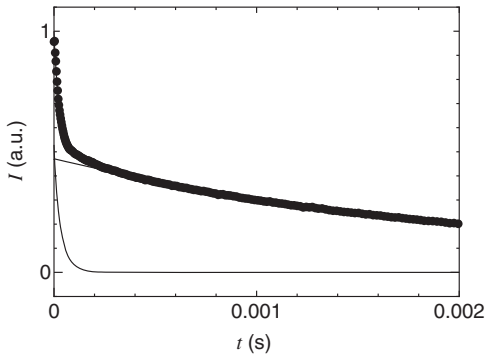

Fig. 2 Normalized spin-spin relaxation function, I, of the relaxation time, t, decomposed into Weibull and exponential functions for a PBS/PEO = 3/7 blend crystallized for 1.341×10^3 s at 48 °C

the crystal growth. The time range of the primary crystallization for PBS was earlier than that for PEO (Fig. 3a). This result is in accordance with that in Fig. 1. PBS, the higher-T_m component, crystallizes before the onset of PEO, the lower-T_m component. The slight increase in f for PEO after the primary crystallization is ascribed to the secondary crystallization. In contrast, the secondary process was almost negligible for PBS.

As displayed in Fig. 3b, the T_2 of PBS was nearly constant throughout the crystallization process, while that of PEO exhibited an increase during the primary process and a decrease during the secondary process. A possible reason for the increase in the primary crystallization process of PEO is its fast crystallization rate, which results in the formation of disordered crystalline structures. The segments in the disordered crystals are expected to have a higher mobility and longer T_2. The slight decrease in T_2 during the secondary process of PEO can be ascribed to the perfection of the PEO crystals. The longer T_2 of PEO compared with that of PBS indicates that the segments in the PEO crystals are more mobile than those in the PBS crystals and that the perfection of the crystals in the secondary process is more apparent for PEO than PBS. However, the nearly constant T_2 of PBS after the primary process indicates that the secondary process is also negligible from the viewpoint of segmental mobility.

Figure 4 shows the changes in f and T_2 for the 3/7 blend crystallized at 48 °C. The results showed a combination of the crystallization behavior of the homopolymers in Fig. 3. The spin-spin relaxation functions of the blends could not be decomposed into the components representing the PBS and PEO crystals because the T_2 values of both components were too close. The value of f first increased in the time range $t \leq ca.\ 10^2$ s and then leveled off, as indicated by line A, before another increase, which is represented by line B. The former and latter increases in f are assigned to the primary crystallization of PBS and PEO, respectively. The secondary crystallization of PBS was also negligible in the blends, whereas the slight increase indicated by line C represents the secondary crystallization of PEO.

As displayed in Fig. 4b, when only PBS crystallized, the crystalline component exhibited a nearly constant T_2, which was comparable with that of the PBS homopolymer in Fig. 3b. After the onset of the primary crystallization of PEO, T_2 varied as seen for the PEO homopolymer in Fig. 3b; it first increased in the primary crystallization process and then slightly decreased in the secondary process of PEO. The increase in T_2 can be ascribed to the longer T_2 of PEO than that of PBS, as indicated in Fig. 3b. The values of f and T_2 as a function of t with the changing T_c are displayed in Fig. 5, and the data for f and T_2 are shifted by 0.2 and decades, respectively. The time range of the crystallization shifted to the right, namely, toward longer t, in Fig. 5 as the T_c increased. Other aspects were nearly independent of the T_c. Note that the induction period of PEO for the blends was longer than that for the homopolymer, which can be ascribed to the dilution effect.

The fractional amount of PBS crystals, f_{PBS} and PEO crystals, f_{PEO}, after the primary crystallization process of each component can be obtained using lines A–C in Fig. 4a. The value of f_{PBS} is indicated by line A, and f_{PEO} can be obtained by subtracting f_{PBS} from f at the intersection point of lines B and C.

Figure 6 shows f_{PBS} as a function of the mass fraction of PBS, w_{PBS}, and T_c. The value of f_{PBS} increased with w_{PBS}. This is simply because the blends with higher PBS contents

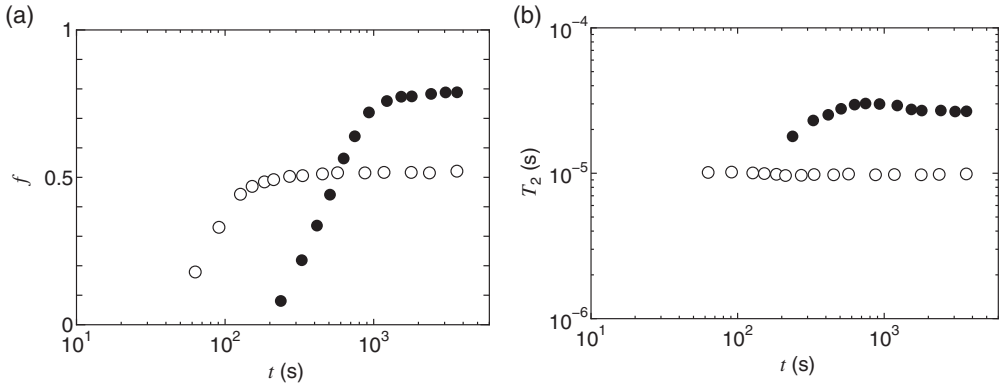

Fig. 3 **a** The fraction of crystals, *f*, and (**b**) the spin-spin relaxation time, T_2, of the PBS (open) and PEO (filled) homopolymers crystallized at 50 °C as a function of the crystallization time, *t*

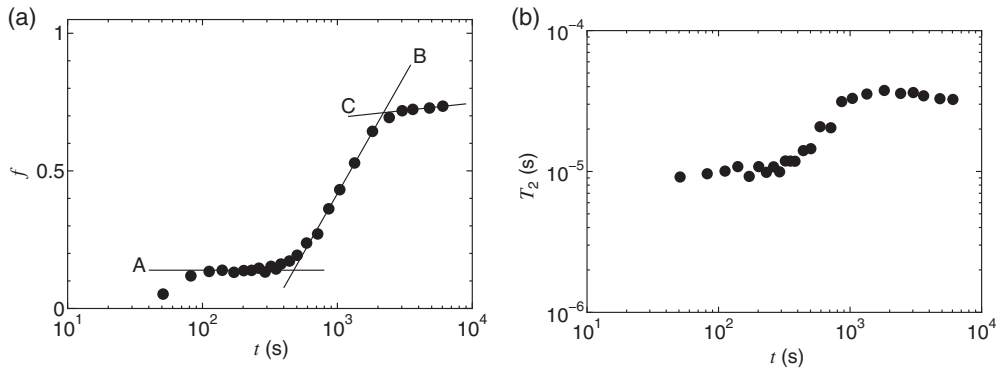

Fig. 4 **a** The fraction of crystals, *f*, and (**b**) the spin-spin relaxation time, T_2, in the PBS/PEO = 3/7 blend crystallized at 48 °C as a function of the crystallization time, *t*. Line A represents the fraction of the crystals after the primary crystallization of PBS. The intersection point of lines B and C represents the fraction of the crystals after the primary crystallization of PEO

contain larger amounts of PBS crystals. In contrast, f_{PBS} was nearly independent of T_c. Figure 7 displays f_{PEO} as a function of the mass fraction of PEO, w_{PEO}, and T_c. As seen for PBS, f_{PEO} increased with w_{PEO}, and it was nearly independent of T_c.

The degree of crystallinity of component *j* (1 for PBS and 2 for PEO), ϕ_j, can be expressed by

$$\phi_j = f_j / F_j \tag{3}$$

where f_j is f_{PBS} or f_{PEO} obtained via pulsed NMR, and F_j is the fractional amount of the protons of component *j*, expressed by

$$F_j = \frac{w_j N_j / M_j}{\sum w_j N_j / M_j} \tag{4}$$

where w_j is the weight fraction, N_j is the number of protons in the repeating unit, and M_j is the molar mass of the repeating unit of component *j*.

Figure 8 displays the degree of crystallinity of PBS, ϕ_{PBS}, as a function of w_{PBS} and T_c. Figure 8a also contains the data for the PBS homopolymer obtained from Fig. 3. The dependence of ϕ_{PBS} on w_{PBS} was completely different from that of f_{PBS}. As w_{PBS} decreased from unity, ϕ_{PBS} first increased and then decreased (Fig. 8a). This result indicates that adding PEO to PBS first enhances and then suppresses the crystallinity of PBS. The value of ϕ_{PBS} is comparable with that of the homopolymer even when w_{PBS} decreased to 0.3. The crystallinity of PBS was suppressed when w_{PBS} was further lowered to 0.2. Figure 8b shows the monotonic decrease in ϕ_{PBS} with the increasing T_c. However, the 2/8 blend did not show a clear dependence on T_c.

Figure 9 indicates the degree of crystallinity of PEO, ϕ_{PEO}, as a function of w_{PEO} and T_c. Figure 9a contains the PEO homopolymer data obtained from Fig. 3. As seen for PBS, the dependence of ϕ_{PEO} on w_{PEO} was completely different from that of f_{PEO}. Although the data points are relatively scattered, they were nearly constant for $0.6 \leq w_{PEO} \leq 1$ and slightly decreased as w_{PEO} further decreased to 0.5. The T_c dependence of ϕ_{PEO} exhibited a monotonic decrease, as seen for PBS. The result in Fig. 9a implies that adding PBS to PEO does not enhance the crystallinity of PEO, which occurs when adding PEO to PBS. Note that the crystallization of PBS reduces the PBS content in the amorphous regions of the PBS spherulites. However, the

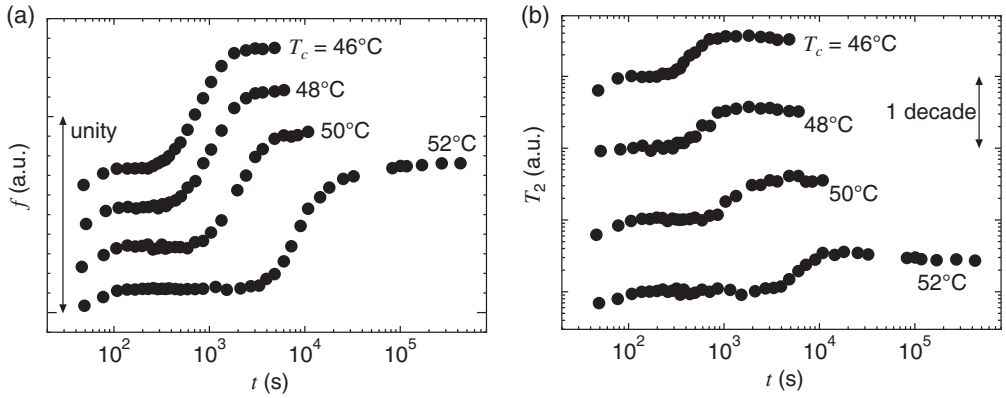

Fig. 5 **a** The fraction of crystals, f, and (**b**) the spin-spin relaxation time, T_2, in the PBS/PEO = 3/7 blend crystallized at various temperatures as a function of the crystallization time, t. The plots were shifted by 0.2 for (**a**) and by decades for (**b**)

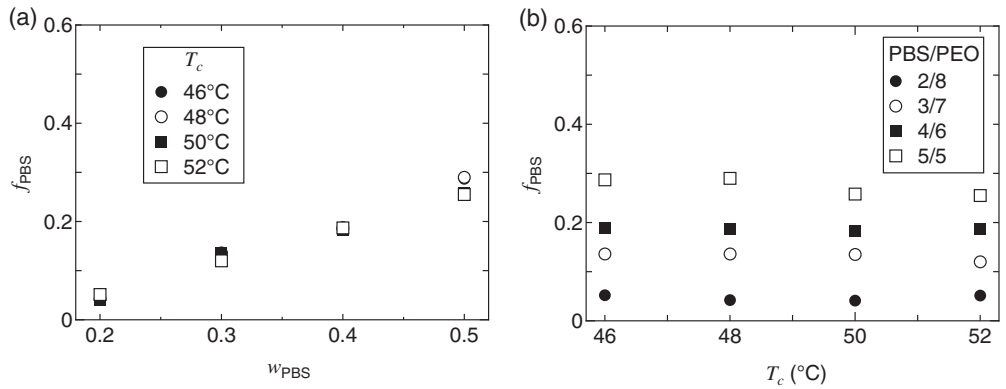

Fig. 6 The fraction of the PBS crystals, f_{PBS}, as a function of (**a**) the weight fraction of PBS, w_{PBS}, and (**b**) the crystallization temperature, T_c

qualitative dependence in Fig. 9a is unchanged because the data points merely shift to the right-hand side of the figure.

The slight decrease in the degree of crystallinity, ϕ, with the increasing T_c for both PBS and PEO (Figs. 8b and 9b, respectively) can be ascribed to the polydispersity of the polymers [34, 37, 44]. The degree of supercooling for the fractions with lower molar masses is further reduced as T_c increases. This is because the polymer with a lower molar mass generally has a lower equilibrium melting point, resulting in a reduced ϕ.

As discussed in other works [34, 45], the behavior of ϕ in crystalline/amorphous blends can be classified into several patterns. Either a monotonic decrease or a maximum is often observed when the content of the amorphous component is increased. In this paper, changing the blend composition induced different influences on the crystallinity of PBS and PEO; Fig. 8a displays a maximum, and Fig. 9a shows the intermediate between the monotonic decrease and the maximum. Note that PEO was still in an amorphous state when PBS crystallized, and un-crystallized PBS acted as the amorphous component when PEO crystallized (note $\phi_{PBS} < 100\%$).

To account for the different behaviors of ϕ_{PBS} and ϕ_{PEO}, at least three factors that affect the crystallinity should be discussed: (i) the dilution effect, (ii) the order of crystallization of the components, and (iii) the difference in the glass transition temperature, T_g. The dilution effect, the first factor, should dominate the reduced crystallinity for $w_{PBS} = 0.2$ and $w_{PEO} = 0.5$, i.e., when the content of each crystallizing component is lower.

The order of crystallization, the second factor, affects the crystallinity of PBS and PEO differently. The crystals of PBS, which crystallize before the onset of the crystallization of PEO, can influence the crystallization process of PEO. When PBS crystallizes, the PEO in the molten state acts as a diluent for the crystallization of PBS. The PEO crystals, which crystallize after PBS, cannot influence the crystallization of PBS. After the spherulitic growth of PBS, PEO molecules are confined in the interlamellar and interfibrillar regions inside the PBS spherulites. [11, 22–24, 33] This leads to suppression of the crystallinity of PEO.

Figure 10 displays ϕ_{PEO} as a function of f_{PBS} and shows a monotonic decrease in ϕ_{PEO} with the increasing f_{PBS}. This result implies that the amount of PBS crystals before the

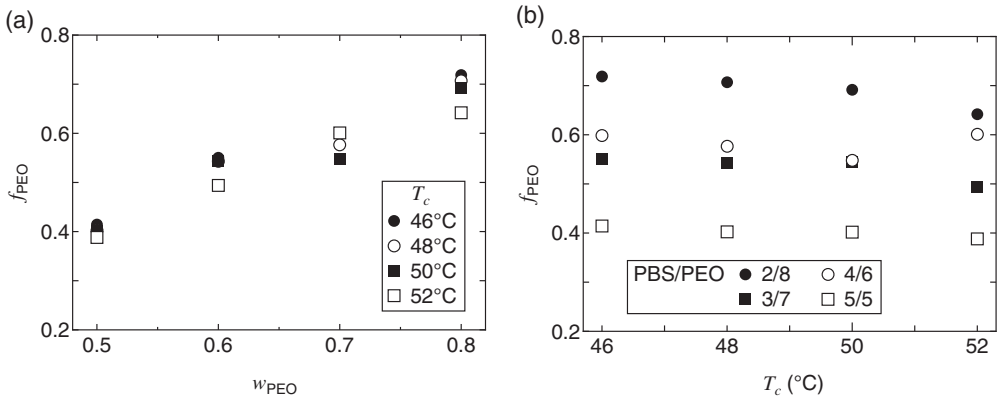

Fig. 7 The fraction of the PEO crystals, f_{PEO}, as a function of (**a**) the weight fraction of PEO, w_{PEO}, and (**b**) the crystallization temperature, T_c

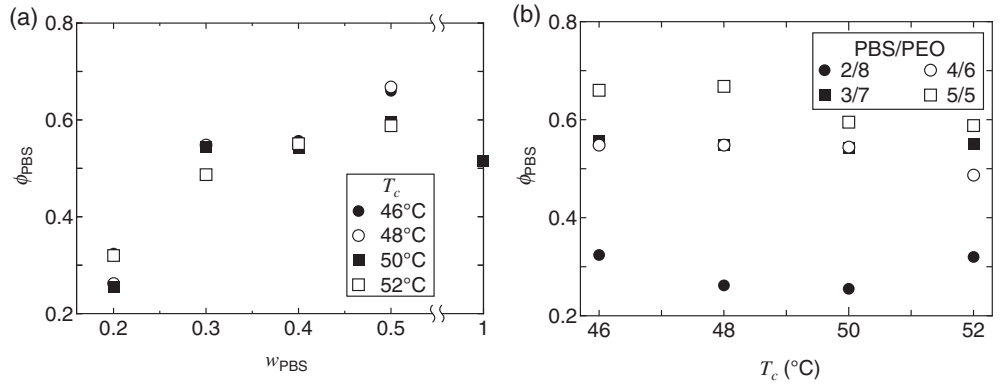

Fig. 8 The degree of crystallinity of PBS, ϕ_{PBS}, as a function of (**a**) the weight fraction of PBS, w_{PBS}, and (**b**) the crystallization temperature, T_c

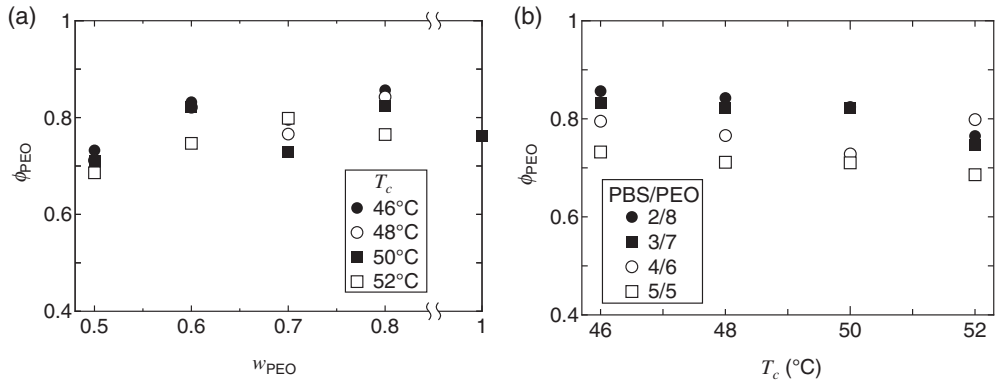

Fig. 9 The degree of crystallinity of PEO, ϕ_{PEO}, as a function of (**a**) the weight fraction of PEO, w_{PEO}, and (**b**) the crystallization temperature, T_c

onset of the crystallization of PEO is actually a factor that influences the crystallinity of PEO. When the blends contain a larger amount of PBS crystals before the onset of the crystallization of PEO, the crystallinity of PEO is further suppressed.

The difference in T_g (the third factor indicated in the former paragraph) can also affect the crystallinity by changing the mobility of the segments. The nucleation rate, I_n, of the polymeric crystals can be expressed by [46]

$$I_n = G_0 \exp\left[-\frac{U}{R(T-T_\infty)}\right] \exp\left(-\frac{K}{k_B T}\right) \quad (5)$$

where G_0 is the constant, U is the activation energy of molecular transport, R is the gas constant, T is the absolute temperature, T_∞ is the temperature at which the motion of the chains is frozen, K is the activation energy of nucleation,

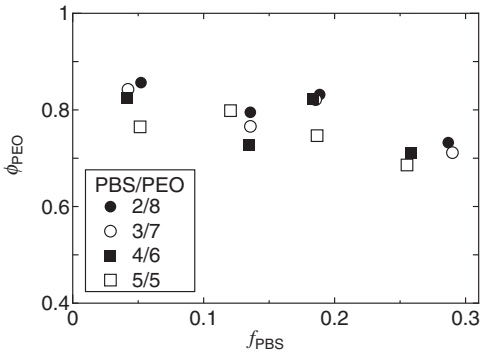

Fig. 10 The degree of crystallinity of PEO, ϕ_{PEO}, as a function of the fraction of the PBS crystals, f_{PBS}

and k_B is the Boltzmann constant. The change in T_g affects T_∞, which is generally approximately 30 K lower than T_g, accounting for nucleation [47]. A miscible blend of PBS and PEO has a single T_g, which is lower and higher than that of the PBS and PEO homopolymers, respectively [19]. Note that PBS is the component with the higher T_g. The change in T_g results in enhanced and suppressed mobility for the segments of PBS and PEO, respectively. According to the first exponential factor in Eq. (5), the change in T_g upon blending enhances the crystallinity of PBS, although I_n and ϕ are different physical quantities.

Conclusions

The degree of crystallinity and the mobility of the PBS and PEO segments in PBS/PEO blends were examined by pulsed NMR. The T_2 data indicated that the mobility of the segments in the PBS crystals was nearly constant throughout the crystallization process. However, the mobility in the PEO crystals first increased in the primary crystallization process and decreased in the secondary crystallization process. The fractional amount of the crystals, f, and the degree of crystallinity, ϕ, exhibited different behaviors. The values of f were dominated by the blend composition. Adding PEO to PBS resulted in an enhancement in ϕ_{PBS}. In contrast, ϕ_{PEO} was nearly constant for $w_{PEO} \geq 0.6$. These results were discussed based on the dilution effect, order of crystallization, and difference in the T_g of the constituents. The dilution effect was apparent when the content of one of the constituents was reduced. PBS crystals, which develop before the onset of the crystallization of PEO, suppressed the crystallinity of PEO, which crystallizes after the completion of the PBS crystallization in the confined regions of the PBS spherulites. The single T_g of the miscible blends can be a factor that contributes to the enhancement of the crystallinity of PBS, i.e., the higher-T_g component.

Acknowledgements The authors thank Mr. Tamotsu Karino for his help with experiments. This work was partly supported by the MEXT-Supported Program for the Strategic Research Foundation at Private Universities, "Creation of new fusion materials by integration of highly ordered nano inorganic materials and ultra-precisely controlled organic polymers".

Compliance with ethical standards

Conflict of interest The authors declare that they have no conflict of interest.

References

1. Blümm E, Owen AJ. Miscibility, crystallization and melting of poly(3-hydroxybutyrate)/poly(l-lactide) blends. Polymer. 1995;36:4077–81.
2. Lee JC, Tazawa H, Ikehara T, Nishi T. Crystallization kinetics and morphology in miscible blends of two crystalline polymers. Polym J. 1998;30:780–9.
3. Ikehara T, Nishi T. Interpenetrated spherulites of poly(butylene succinate)/poly(vinylidene chloride-co-vinyl chloride) blends. An optical microscopic study. Polym J. 2000;32:683–7.
4. Qiu Z, Ikehara T, Nishi T. Unique morphology of poly(ethylene succinate)/poly(ethylene oxide) blends. Macromolecules. 2002;35:8251–4.
5. Terada Y, Ikehara T, Nishi T. Direct observation of the interpenetrated spherulites by atomic force microscopy. Polym J. 2000;32:900–3.
6. Ikehara T, Nishikawa Y, Nishi T. Evidence for the formation of interpenetrated spherulites in poly(butylene succinate-*co*-butylene carbonate)/poly(l-lactic acid) blends investigated by atomic force microscopy. Polymer. 2003;44:6657–61.
7. Lu J, Qiu Z, Yang W. Effects of blend composition and crystallization temperature on unique crystalline morphologies of miscible poly(ethylene succinate)/poly(ethylene oxide) blends. Macromolecules. 2008;41:141–8.
8. He S, Liu J. Crystallization and morphology development of binary crystalline poly(ethylene succinate)/poly(ethylene oxide) (pes/peo) blend with non-isothermal crystallization. Polym J. 2007;39:537–42.
9. Wang H, Zhao T, Wang X, Guo P, Ren L, Qiang T, Luo X, Qiang X. Effects of crystallization condition of poly(ethylene succinate) on the crystallization of poly(ethylene oxide) in their blends. Polym Bull. 2012;69:955–65.
10. Li Q, Liu J. Morphology and interpenetrated growth of spherulites in miscible poly(ethylene succinate)/poly(ethylene oxide) blends. Colloid Polym Sci. 2013;291:2007–12.
11. Ikehara T, Kurihara H, Kataoka T. Spherulitic growth in block copolymers and blends of miscible crystalline polymers. J Polym Sci Part B Polym Phys. 2012;50:563–71.
12. Nozue Y, Hirano S, Kawasaki N, Ueno S, Yagi N, Nishi T, Amemiya Y. Penetration of PBSU spherulite into P(VDC-VC) spherulite observed with microbeam- and macro beam-SAXS/WAXS measurements. Polymer. 2004;45:8593–601.
13. Weng M, Qiu Z. A spherulitic morphology study of crystalline/crystalline polymer blends of poly(ethylene succinate-co-9.9 mol % ethylene adipate) and poly(ethylene oxide). Macromolecules. 2013;46:8744–7.
14. Zeng J-B, Zhu Q-Y, Li Y-D, Qiu Z-C, Wang Y-Z. Unique crystalline/crystalline polymer blends of poly(ethylene succinate) and poly(p-dioxanone): miscibility and crystallization behaviors. J Phys Chem B. 2010;114:14827–33.

15. Hirano S, Terada Y, Ikehara T, Nishi T. Observation of interpenetrated spherulites by confocal laser scanning microscopy. Polym J. 2001;33:371–3.
16. Ikehara T, Kimura H, Qiu Z. Penetrating spherulitic growth in poly(butylene adipate-*co*-butylene succinate)/poly(ethylene oxide) blends. Macromolecules. 2005;38:5104–8.
17. Ye L, Ye C, Xie K, Shi X, You J, Li Y. Morphologies and crystallization behaviors in melt-miscible crystalline/crystalline blends with close melting temperatures but different crystallization kinetics. Macromolecules. 2015;48:8515–25.
18. Jiang N, Abe H. Miscibility and morphology study on crystalline/crystalline partially miscible polymer blends of 6-arm poly(llactide) and poly(3-hydroxybutyrate-co-3-hydroxyvalerate). Polymer. 2015;60:260–6.
19. Qiu Z, Ikehara T, Nishi T. Miscibility and crystallization in crystalline/crystalline blends of poly(butylene succinate)/poly (ethylene oxide). Polymer. 2003;44:2799–806.
20. Ikehara T, Kurihara H, Kataoka T. Effect of poly(butylene succinate) crystals on spherulitic growth of poly(ethylene oxide) in binary blends of the two substances. J Polym Sci Part B Polym Phys. 2009;47:539–47.
21. Qiu Z, Ikehara T, Nishi T. Melting behaviour of poly(butylene succinate) in miscible blends with poly(ethylene oxide). Polymer. 2003;44:3095–9.
22. Wang H, Schultz JM, Yan S. Study of the morphology of poly (butylene succinate)/poly(ethylene oxide) blends using hot-stage atomic force microscopy. Polymer. 2007;48:3530–9.
23. Ikehara T, Kurihara H, Qiu Z, Nishi T. Study of spherulitic structures by analyzing the spherulitic growth rate of the other component in binary crystalline polymer blends. Macromolecules. 2007;40:8726–30.
24. He Y, Zhu B, Kai W, Inoue Y. Effects of crystallization condition of poly(butylene succinate) component on the crystallization of poly(ethylene oxide) component in their miscible blends. Macromolecules. 2004;37:8050–6.
25. Hirano S, Nishikawa Y, Terada Y, Ikehara T, Nishi T. Miscibility and crystallization behavior of crystalline/crystalline polymer blends. poly(ester carbonate)/poly(l-lactic acid). Polym J. 2002;34:85–88.
26. Qiu Z, Fujinami S, Komura M, Nakajima K, Ikehara T, Nishi T. Spherulitic morphology and growth of poly(vinylidene fluoride)/poly(3-hydroxybutyrate-*co*-hydroxyvalerate) blends by optical microscopy. Polymer. 2004;45:4355–60.
27. Qiu Z, Yan C, Lu J, Yang W. Miscible crystalline/crystalline polymer blends of poly(vinylidene fluoride) and poly(butylene succinate-co-butylene adipate): spherulitic morphologies and crystallization kinetics. Macromolecules. 2007;40:5047–53.
28. Qiu Z, Chunzhu Yan C, Lu J, Yang W, Ikehara T, Nishi T. Various crystalline morphology of poly(butylene succinate-co-butylene adipate) in its miscible blends with poly(vinylidene fluoride). J Phys Chem B. 2007;111:2783–9.
29. Ikehara T, Kimura H, Kataoka T. Miscibility enhancement and formation of interpenetrating spherulites in ternary blends of crystalline polymers. J Polym Sci Part B Polym Phys. 2010;48:706–11.
30. Wang T, Li H, Wang F, Yan S, Schultz JM. Confined growth of poly(butylene succinate) in its miscible blends with poly(vinylidene fluoride): morphology and growth kinetics. J Phys Chem B. 2011;115:7814–22.
31. Wang H, Feng H, Wang X, Du Q, Yan C. Crystallization kinetics and morphology of poly(vinylidene fluoride)/poly(ethylene adipate) blends. Chin J Polym Sci. 2015;33:349–61.
32. Bai S, Wang Q. Miscible crystalline/crystalline polymer blends of polyoxymethylene copolymer/poly(ethylene oxide) with interpenetrated spherulites and enhanced properties. J Vinyl Addit Tech. 2016;22:479–86.
33. Stein RS, Khambatta FB, Warner FP, Russell T, Escala A, Balizer EJ. X-ray and optical studies of the morphology of polymer blends. J Polym Sci Polym Symp. 1978;63:313–28.
34. Ikehara T, Ito D, Kataoka T. Analysis of the degree of crystallinity in interpenetrating spherulites of poly(ethylene succinate) and poly(ethylene oxide) blends using pulsed NMR. Polym J. 2015;47:379–84.
35. He Z, Liang Y, Wang P, Han CC. Effect of lower critical solution temperature phase separation on crystallization kinetics and morphology of poly(butylenes succinate)/poly(ethylene oxide) blend. Polymer. 2013;54:2355–63.
36. Tanaka H, Nishi T. Study of crystallization process of polymer from melt by a real-time pulsed NMR measurement. J Chem Phys. 1986;85:6197–209.
37. Ikehara T, Nishi T. Primary and secondary crystallization processes of poly(ϵ-caprolactone)/styrene oligomer blends investigated by pulsed NMR. Polymer. 2000;41:7855–64.
38. Fujimoto K, Nishi T, Kado R. Multiple-pulse nuclear magnetic resonance experiments on some crystalline polymers. Polym J. 1972;3:448–62.
39. Kitamaru R, Horii F, Hyon S-H. Proton magnetic resonance studies of the phase structure of bulk-crystallized linear polyethylene. J Polym Sci Polym Phys. 1977;15:821–36.
40. McBrierty VJ, Douglass DC. Recent advances in the NMR of solid polymers. J Polym Sci Macromol Rev. 1981;16:295–366.
41. McBrierty VJ, Douglass DC. Nuclear magnetic resonance of solid polymers. Phys Rept. 1980;63:61–147.
42. Douglass DC, McBrierty VJ, Weber TA. Anisotropic motional averaging in a constrained polymer chain. J Chem Phys. 1976;64:1533–7.
43. Powles JG, Strange JH. Zero time resolution nuclear magnetic resonance transient in solids. Proc Phys Soc. 1963;82:6–15.
44. Gornick F, Mandelkern L. Effect of noncrystallizable components on the crystallization kinetics of polymers. J Appl Phys. 1962;33:907–13.
45. Paul DR, Barlow JW. Crystallization from miscible polymer blends. In: Klempner D, Frisch KC, editors. Polymer Alloys II: blends, blocks, grafts, and interpenetrating networks. New York, NY: Plenum; 1980. pp. 239–53.
46. Mandelkern L, Crystallization of polymers. 2nd edn, Vol. 2. UK, Cambridge; 2004.
47. Runt JP. Crystalline Polymer Blends. In: Paul DR, Backnall CB, editors. Polymer Blends, Vol. 1, Chapter 6. New York, Wiley; 2000. pp. 167–86.